Available online at www.sciencedirect.com

ScienceDirect

Energy Procedia 00 (2017) 000–000

Energy Procedia

www.elsevier.com/locate/procedia

7th International Conference on Silicon Photovoltaics, SiliconPV 2017

Selectivity issues of MoO_x based hole contacts

Lisa Neusel[a]*, Martin Bivour[a], Martin Hermle[a]

[a]*Fraunhofer Institute for Solar Energy Systems ISE, Heidenhofstrasse 2, 79110 Freiburg, Germany,*

Abstract

Evaporated MoO_x was investigated as hole contact for silicon solar cells. To improve understanding of the carrier selectivity of metal oxide based hole contacts the *J-V* characteristic of simple MoO_x-based solar cells was evaluated and different pre and post deposition treatments as well as the influence of the buffer layer for solar cell like precursors were investigated. Further on, the loss of selectivity with annealing was investigated with the same set of samples. While characteristic changes of the optical properties by some treatments indicated the modification of the metal oxides gap states, a clear correlation with the electrical junction properties was not observed. Since none of those treatments showed a beneficial influence on carrier selectivity, further work is needed towards an efficient engineering of the selectivity. However, evaluation of various data showed that the loss of selectivity with annealing is governed by a reduced effective work function of the TMOs.

Peer review by the scientific conference committee of SiliconPV 2017 under responsibility of PSE AG.

Keywords: Transition metal oxides; molybdenum oxide; selectivity; work function; induced bend bending; silicon heterojunction

1. Introduction

Transition metal oxides (TMOs) like MoO_x and WO_x are currently investigated as alternative selective hole contact materials for silicon solar cells [1,2]. Due to their high work function, a band bend bending and pn-junction are induced in the silicon absorber, leading to a hole selective contact. Further on, the low parasitic absorption in the blue wavelength region offers the potential of higher J_{sc} than selective hole contacts based on doped silicon layers

* Corresponding author. Tel.: +49 761/4588-5921
E-mail address: Lisa.Neusel@ise.fraunhofer.de

Peer review by the scientific conference committee of SiliconPV 2017 under responsibility of PSE AG.

(e.g. a-Si or poly-Si) [2]. However, one major problem of those novel contact materials is their higher sensitivity towards low-temperature annealing leading to *FF* and V_{oc} losses. While the origin of those losses is not well understood so far, it is clear that they cannot be described with the classical one diode model and the losses within this simple model (recombination, ohmic transport, ohmic shunts). These losses result from a non-ideal hole selectivity of the used TMOs due to non-ideal hole extraction from the absorber.

Fig. 1 shows the improved blue response if the a-Si:H(p) (black) at the front side of a SHJ solar cell is replaced by MoO_x (green) or WO_x (blue). This main advantage of the TMOs – the reduced band gap absorption due to their high optical band gap – comes along with two major challenges of MoO_x and WO_x: Besides the poor temperature stability, parasitic absorption for wavelengths above 600 nm is observed. The latter is caused by gap states [3,4] which define the optical and electrical properties of TMOs to a great extent [5,6]. These states are of great importance and well-studied for the gas-, electro-, and photochromic properties of TMOs [5] utilized for various application (sensing, smart windows, ...). However, their relevance for the carrier selectivity, e.g. the conductivity, effective work function and gap states which might be essential for providing an efficient transport path for the hole extraction from the absorber, is explored mainly for organic electronics [6–8]. Regarding the electrical performance of the cells from Fig. 1 it is observed that annealing has a strong influence on the selectivity and therefore *FF* and V_{oc} [2]. For example, a higher efficiency owing to improved optical and electrical properties is observed if a-Si:H(p) is replaced by MoO_x. However, annealing degrades the initial good selectivity which is reflected by a S-shaped *J-V* characteristic and a drop in *FF* and V_{oc} [2,9]. So far, it is speculated that hydrogen from the a-Si:H(i) buffer and reduced c-Si band bending [2] or the deposition of the TCO electrode [9] play a crucial role.

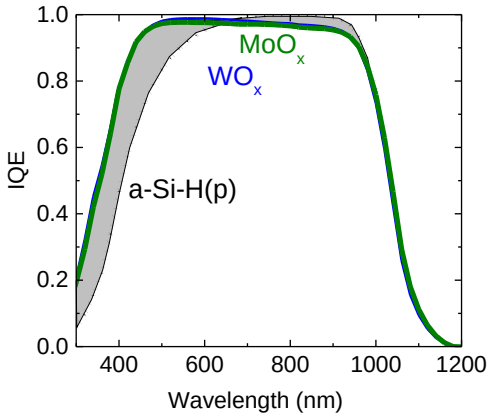

Fig. 1. IQE of SHJ cells with different thin film metal oxides at the front forming the hole contact. For a detailed discussion of those different hole contact materials see [10].

The objective of this paper is to shed some light on the selectivity related issues and the degradation of the solar cell performance. Firstly, the influence of the TMO thickness is investigated to reduce optical losses (Sec. 3.1). In the course of this optimization the influence of the a-Si:H(i) buffer on the selectivity is examined and the non-ideal carrier extraction for cells with buffer layer is described (Sec. 3.2). The second part focuses on the analysis of different treatments before and after the MoO_x deposition on solar cell like test structures for a simple and fast characterization concerning selectivity losses (Sec. 3.4 and 3.5). Here the role of hydrogen from the a-Si:H(i) buffer and the influence of different plasma treatments after the TMO deposition are investigated - with the aim to gain further knowledge about possible modifications of MoO_x and a basic understanding for engineering the TMOs towards improved selectivity.

2. Experimental details

The first part of this paper (Sec. 3.1) deals with the evaluation of simple planar front emitter solar cells with various MoO_x thicknesses as shown in Fig. 2a. In the second part the MoO_x films are investigated with solar cell like test structures as shown in Fig. 2b (QSSPC and Suns-V_{oc} samples). Their fabrication which only slightly differs from

the fabrication of the solar cells with respect to the contact metallization is outlined in the following. A schematic of the samples for an optical characterization with reflection and transmission measurements can be seen in Fig. 2c.

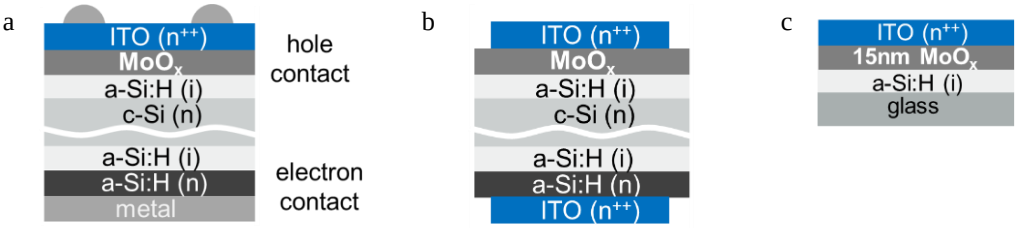

Fig. 2. (a) Simple planar front emitter solar cells; (b) Solar cell like test structures - so called QSSPC and Suns-Voc samples; (c) Structures on glass for optical characterization.

2.1. Solar cells

The deposition of the MoO_x films of various thicknesses (6.5 nm, 8.4 nm, 9.9 nm, 15.3 nm) was performed by thermal evaporation from stoichiometric powder. The ITO was deposited by reactive sputtering and its thickness was adapted to obtain a similar reflection for all investigated front sides. To examine the influence of the a-Si:H(i) buffer layer cells with ~10 nm MoO_x were fabricated with and without buffer (~8.5 nm) at the front side. The front side was finished by a metal grid electrode (e-beam evaporated Ti/Pd/Ag) which was structured by photolithography and the lift-off technique. Unlike for screen-printed metal contacts, no final annealing step is needed to lower the series resistance R_s for the evaporated grid electrode. The active cell area (2 x 2 cm^2) was defined by using a shadow mask during ITO deposition. Further details can be found in [2].

The results are shown before and after and annealing at different temperatures for 15 minutes on a hotplate in ambient air. A minimum temperature of 180 °C is typically needed to activate the surface passivation by a-Si:H(i). However, such temperatures might also be needed during the back end processing for metallization, TCO deposition or TCO post crystallization and the module integration [10].

2.2. Sample preparation: Test structures

The fabrication of the test structures (small area solar cell precursors) for QSSPC, Suns-V_{oc} and surface photovoltage (SPV) measurements is very similar to the fabrication of the solar cells. Only the final metallization step is missing and differs from that of the cells as a 70 nm thick ITO layer is used also at the rear. The MoO_x thickness for all test structure results presented in this paper was chosen to approximately 6.5 - 7.5 nm as cells with this thickness revealed the lowest *FF* degradation with annealing (see Fig. 3a).

For an evaluation of the optical properties glass samples, as shown in Fig. 2c, were fabricated and transmission and reflection measurements were conducted with the spectrophotometer *Varian Cary 5000*. Therefore thin glass substrates (Carl Roth GmbH & Co, borosilicate) were used. For higher signal sensitivity the MoO_x thickness for the glass structures was chosen to about 15 nm. To prevent blistering of the ITO layer the heat up time in the sputter chamber before the deposition was extended compared to cells and cell precursors. Different annealing steps for those structures were also conducted for 15 minutes on a hotplate in ambient air.

The plasma treatments of Sec. 3.5 were performed with the plasma cluster for etching SI 600 from SENTECH with a microwave (MW) slot-antenna (SLAN) excitation source (2.45 GHz). For the Argon, hydrogen and oxygen plasma treatments a minimal ECR-power of 750 W which still ensures stable plasma, a pressure of 20 Pa and gas flow of 50 sccm were set. The maximal possible gas flow for carbon dioxide was 37 sccm.

2.3. Measurements

Typical solar cell characterization consists of measuring the *J-V* characteristic at STC conditions (1000 W/m^2, 25 °C, AM1.5 g) with an in house set up. For more detailed investigations the temperature (15-70 °C) dependence of

the *J-V* characteristic was analyzed with the LOANA systems from pv-tools [11]. The latter setup was also used for quantum efficiency measurements. Further details can be found in [12].

Quasi Steady-State Photo Conductance (QSSPC) measurements were done with a WCT120 tester from Sinton Instruments. For Suns-V_{oc} measurements also a setup from Sinton Instruments (Sinton III) was used. Surface photovoltage measurements to measure the induced c-Si dark band bending were done with an in house set up.

3. Results and discussion

3.1. Reduction of optical losses on solar cell level: Influence of MoO_x thickness

In this section at first only results for cells with an a-Si:H(i) buffer layer are regarded. As mentioned in the introduction (Fig. 1) parasitic sub-band gap absorption in MoO_x leads to losses between 600 nm and 1000 nm which are not observed for the p-type a-Si:H. Looking at the short circuit current density (J_{sc}, Fig. 3b) of the solar cells a linear decrease with the metal oxide thickness can be observed: MoO_x-based cells with a structure like in Fig. 2a experience current density losses of about 0.1 mA/cm^2 per nm in the as deposited state. A similar trend is observed for an annealing series from 150 °C to 330 °C.

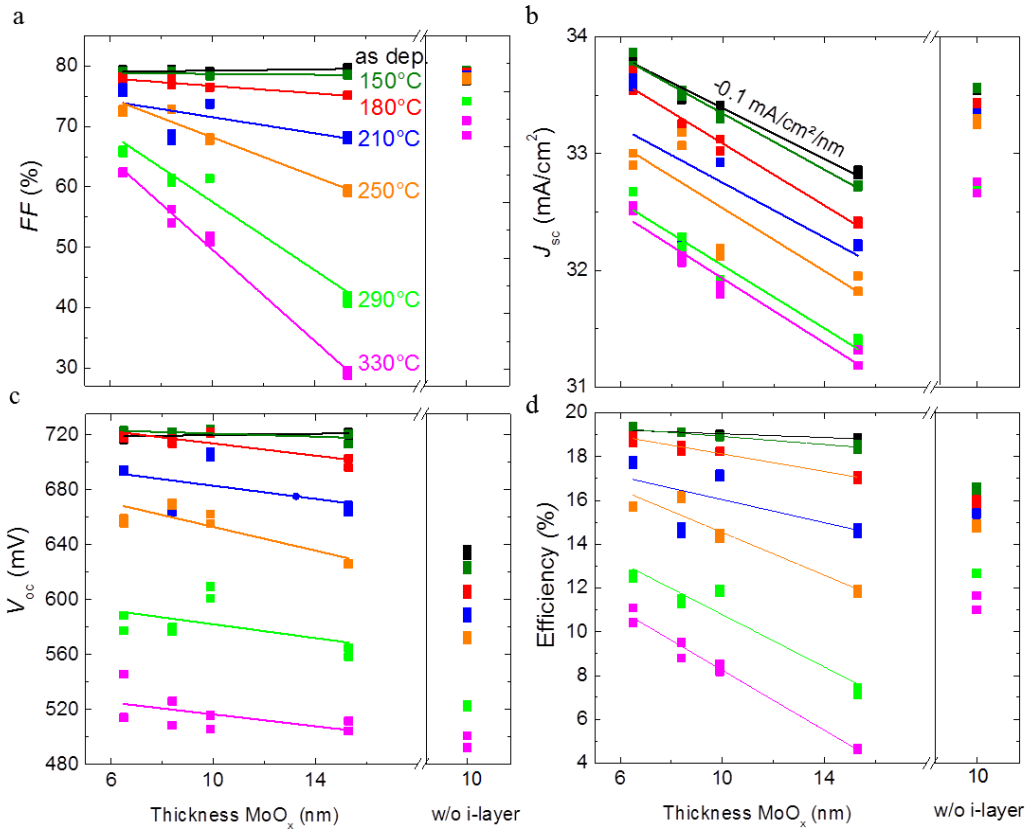

Fig. 3. Cell results for different MoO_x thicknesses as deposited and for an annealing series from 150 °C to 330 °C for 15 minutes, respectively.

Fig. 4 provides more information on the influence of the MoO_x thickness on the parasitic absorption and it can be seen that that the lower EQE and hence J_{sc} for the thickest MoO_x film (15.3 nm, red curve) are caused by lower IQE due to higher sub-band gap absorption between 600 nm and 1000 nm. This shows that these losses are significant and that the thickness of the metal oxides has to be reduced to a minimum. However it can also be seen that the reflection is increased for thicker films which is a result of non-ideally adapted ITO thickness.

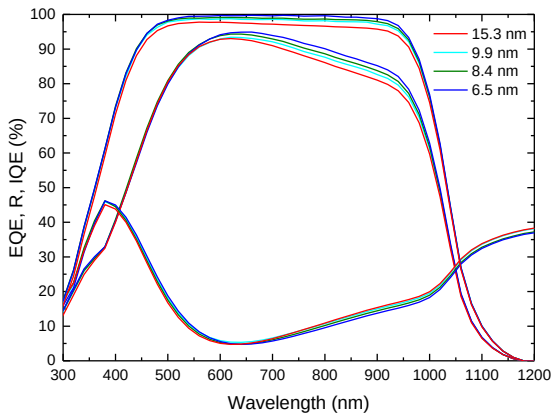

Fig. 4. External quantum efficiency (EQE), internal quantum efficiency (IQE) and reflection (R) for cells with various MoO_x thicknesses.

3.2. FF losses: Influence of MoO_x thickness and a-Si:H(i) buffer

Regarding the electrical properties in Fig. 3a for cells with an a-Si:H(i) buffer layer, it can be seen that even for a very thin MoO_x film of only 6.5 nm still high *FF*s close to 80 % are achieved in the as deposited state. However a strong *FF* degradation with increasing annealing temperature is visible which is much more pronounced for increasing MoO_x thicknesses. For temperatures relevant during the solar cell manufacturing process (below 200 °C) the degradation is less distinct: For the cell with about 6.5 nm thick MoO_x a *FF*-drop of about 1 % is observed after the final annealing step at 180 °C.

Another interesting point is that not only the metal oxide thickness but also the presence of the a-Si:H(i) buffer leads to *FF* degradation with annealing. However, omitting the buffer layer is not device relevant, as those cells show poor surface passivation which limits the extractable voltage V_{oc} and the efficiency (Fig. 3c). In Fig. 3a it can be seen that the *FF* loss for the 10 nm MoO_x film is less pronounced without the buffer layer. One hypothesis is that hydrogen effusion from the buffer somehow modifies the metal oxide [2], which is further investigated in Sec. 3.4. Another hypothesis is that annealing results in the formation of an interlayer between MoO_x and TCO which influences the degradation behavior [9].

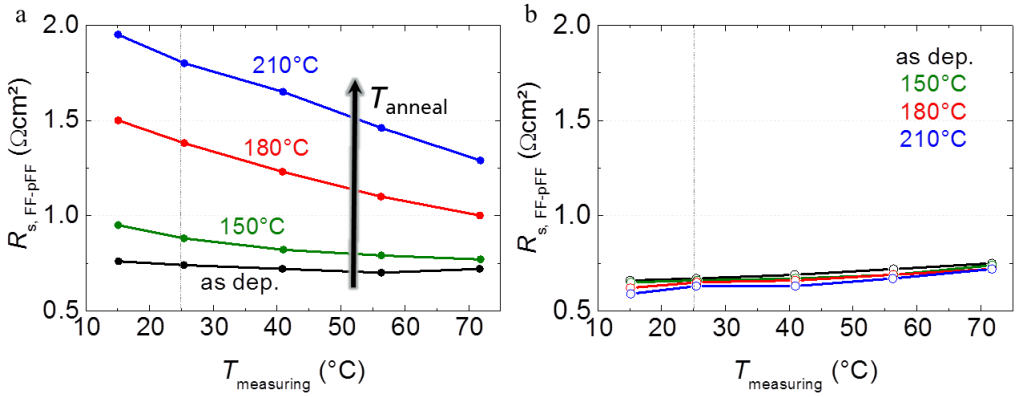

Fig. 5. Temperature dependence of transport related losses with the series resistance as characteristic measure. R_s is plotted as a function of the measuring temperature and results for a final annealing series from 150 °C to 210 °C are shown for the 10 nm thick MoO_x-based cells with i-buffer (a) and without i-buffer (b).

For a deeper understanding towards the influence of the a-Si:H(i) buffer on the *FF* degradation with annealing and to clarify to what extent this impacts hole collection of such devices, the temperature dependence of the series

resistance (R_s) for the cells with the 10 nm thick MoO_x is analyzed. R_s - extracted from the *FF* and pseudo *FF* [13] is plotted in Fig. 5a and b as a function of the measuring temperature (15 – 70 °C) for a cell with and without buffer layer annealed from 150 °C to 210 °C, respectively. In accordance with the *FF*s in Fig. 3a a significant increase in R_s at 25°C is observed with increasing annealing temperature for the cell with buffer (Fig. 5a) which is not the case without the buffer. Not only a higher R_s at 25 °C but also a strong temperature dependence is observed. The higher R_s and its reduction with increasing measuring temperature can be explained by a thermally activated transport which is needed for overcoming the higher transport barriers for higher annealing temperatures for which tunneling is not efficient anymore. The described behavior therefore indicates that it is not a classical series resistance showing ohmic characteristic for the case with buffer. It reveals that a non-ideal selectivity due to non-ideal hole extraction is obtained if MoO_x is combined with the a-Si:H(i) buffer.

3.3. Simple approach to probe selectivity with test structures

To take into account that the characteristic and losses of such non-optimized contacts might not obey the classical diode law a characterization approach adapted from Ref. [12] is used. It is based on the relatively simple current-less measurements of the induced c-Si equilibrium band bending (V_{bb} in Fig. 6), the external V_{oc} and the implied V_{oc} (iV_{oc}) of simple small area solar cell precursors. It allows identifying whether the passivation (iV_{oc}) or an insufficient selectivity is dominating the electrical losses of the investigated contact. By comparing the V_{oc} from Suns-V_{oc} measurements and iV_{oc} from QSSPC measurements we probe whether the contact fulfills one basic requirement of the diode theory [14–16], which is a negligible gradient in the Fermi-level of the contact's majority carriers. Accordingly, $\Delta V = iV_{oc}$-$V_{oc} > 0$ eV (Fig. 6) will indicate that the characteristic of the contact is determined by an insufficient selectivity, i.e. a "non-ideal" rectifying behavior. We have found it useful to use ΔV as a figure of merit for the contact´s selectivity and a selection criterion for further investigations, e.g. to justify investigations on solar cell level.

V_{bb} is measured by the surface photo-voltage technique and gives valuable information on the inversion of the c-Si surface and the corresponding induced c-Si junction which is of major importance for the selectivity of such induced junctions [17,18]. Thus, V_{bb} provides indirect information on the effective work function and the charges causing the inversion and hence the asymmetric hole / electron conductivity needed for a negligible gradient in the Fermi-level of the contact's majority carriers during operation [15].

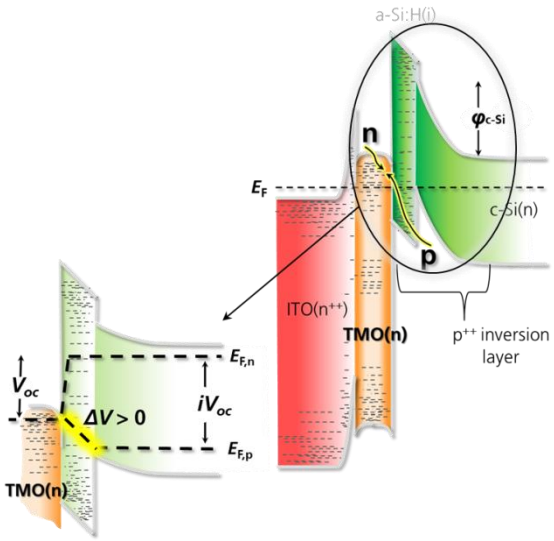

Fig. 6. Sketch of the band diagram (right: in equilibrium, left: during operation) of a TMO-based heterojunction solar cell to visualize the two important parameters for a characterization of non-ideal hole selectivity: The induced c-Si dark bend bending $\varphi_{c\text{-}Si}$ (V_{bb}) and voltage loss ΔV due to insufficient carrier selectivity.

The basic suitability of this approach is now determined by comparing V_{bb} and ΔV for test structures as described in Sec. 2.2. In the two graphs in Fig. 7 V_{bb} and ΔV are plotted over the annealing temperature. For a reference cell with doped amorphous silicon (a-Si:H(p) ~ 7 nm) a slight improvement with annealing and no problems with selectivity occurs - a behavior also appearing for the *FF*, which slightly increases for the first annealing steps [10]. For a replacement of the a-Si:H(p) with MoO_x a similar behavior comparable to the *FF* degradation on solar cell level from Sec. 3.2 is observed: A reduced band bending with annealing appears which is more pronounced with buffer (black vs. grey, Fig. 7a). Furthermore also a loss of selectivity occurs for the two structures with MoO_x and at least for higher annealing temperatures it is more pronounced for the cell with buffer layer (Fig. 7b). The reference shows no selectivity issues since ΔV is close to zero. This substantiates that the observed behavior of the series resistance after annealing with buffer layer in Sec. 3.2 is a result of non-ideal contact selectivity.

3.4. Annealing of a-Si:H(i) before MoO_x deposition

As mentioned before one hypothesis is, that hydrogen effusing from the a-Si:H(i) buffer layer causes the loss of selectivity during annealing. To modify the hydrogen release during the final annealing steps the precursors with a-Si:H(i) buffer were annealed before the MoO_x deposition at 210 °C (red, Fig. 7) and 300 °C (blue, Fig. 7).

A comparison of the results in Fig. 7a and b reveals a similar behaviour for the samples with the pre-annealed buffer layers (red, blue) compared to the untreated one (black) as V_{bb} and ΔV decrease in a similar way. This is somewhat unexpected concerning the proposed role of hydrogen since at least for the buffer pre-annealed at 300 °C (blue) it is expected that a significant amount of hydrogen is already released before the MoO_x deposition and hence a substantial lower amount of hydrogen could effuse into the MoO_x layer during the final annealing steps which are performed at much lower temperatures. It can accordingly be concluded that with this experiment the hypothesis of a modification of MoO_x by hydrogen from the buffer could not be confirmed.

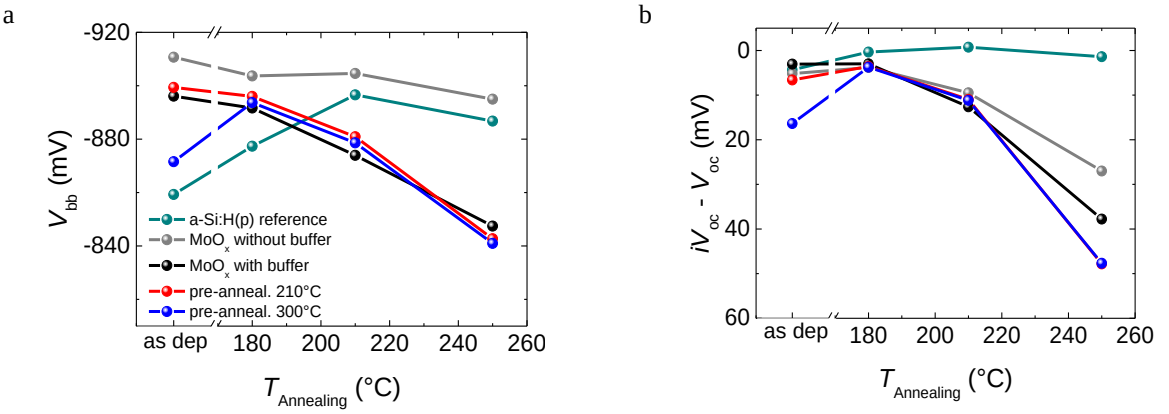

Fig. 7. (a) Induced c-Si band bending and (b) $\Delta V = iVoc\text{-}Voc$ for a reference with a-Si:H(p) and MoO_x test structures with and without a-Si:H(i) buffer layer and for different buffer pre-annealing temperatures vs. the final transient annealing from 180 °C up to 250 °C.

3.5. Post deposition treatment of MoO_x

In a next step we tried to modify the metal oxides stoichiometry on purpose to gain further knowledge about the materials' properties for engineering the TMOs towards improved selectivity. Various publications already proposed that changing the stoichiometry of TMOs via formation of gap states also influences their electrical properties [3,4,8], which is actually utilized for various application (sensing, smart windows, ...). In this sense, different post deposition treatments of MoO_x were done for the samples in Fig. 2c with the basic idea to probe whether the occurrence of gap states in the metal oxide is linked to the observed selectivity losses. First it was examined how the MoO_x is modified by annealing. In the course of this, another method to analyze the optical properties was utilized: Measuring the absorption spectrum of i/ MoO_x/ ITO structures on glass (see Sec. 2.2). The results in Fig. 8a reveal that sub-band gap defects are formed with annealing, resulting in an absorption peak at around 800 to 1000 nm. This generally fits to the loss of selectivity observed with annealing at 180 °C (black curve, Fig. 7 and Fig.

8c) and could imply a link between gap states formed by annealing and selectivity losses. However, for 210 °C and 250 °C rather a slight reduction of the sub-band gab absorption and hence re-oxidation, in accordance with results from Werner et al [4] is observed, which is in contrast to the continuously decreasing selectivity ΔV with annealing for the black curve in Fig. 8c.

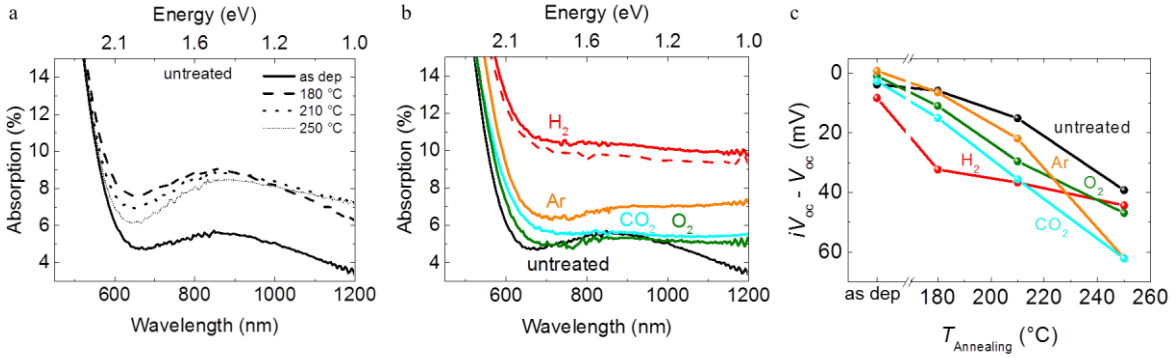

Fig. 8. Influence on absorbance by a) annealing and b) plasma treatment of the test structures. c) Influence of plasma treatment on selectivity.

In addition to annealing, different post deposition plasma treatments were applied to modify the MoO_x properties before the ITO deposition for the samples shown in Fig. 2c. The successful modification of the gap states is apparent from the absorption features for the films on glass (Fig. 8b) which are similar to those from Ref. [4] and [3]. For hydrogen (red) the reduction of the metal oxide causes gap states resulting in an increased absorption. A further reduction by an additional annealing at 180 °C is not observed (red, dashed line). Argon plasma (orange) only shows a slight increase in absorption. Oxygen (green) and carbon dioxide (cyan) plasma was checked as well with the intension to get a more stoichiometric material, but no further oxidation or improvement concerning sub band gap absorption can be observed.

Concerning selectivity ΔV, Fig. 8c reveals no remarkable difference for the different plasma treatments in the as deposited state and especially with annealing no improvement compared to the untreated MoO_x reference is observed. While hydrogen plasma has a slight detrimental influence on the selectivity, Argon, O_2 and CO_2 plasma also show no beneficial impact. Considering the results from Fig. 8b, at least for the reduction and pronounced absorption peak of MoO_x by the H_2 plasma, a more significant decrease in ΔV in the as deposited state would be expected. Additionally, a slight decrease in absorption is observed for annealing the H_2 treated sample at 180°C (dashed red), while ΔV further decrease. Hence, it can be concluded that no direct correlation between the gap states formed during annealing or by the plasma treatments and the selectivity exists for this experiment.

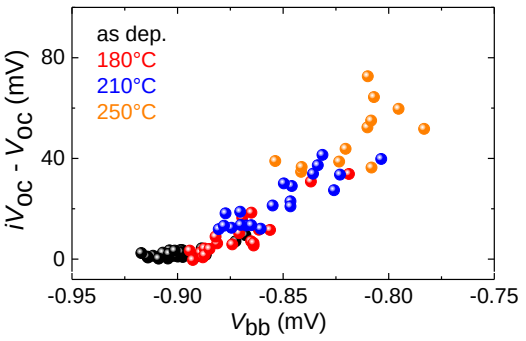

Fig. 9. Dependence of selectivity on the induced c-Si band bending for different annealing temperatures.

Fig. 9 summarizes data from various investigations. It can be seen that the selectivity is governed by the induced c-Si band bending and that the loss of selectivity with annealing is caused by a reduction of the band bending (linear dependence between V_{bb} and ΔV). This highlights the importance for the engineering of the effective work function

and/or the (negative) charges at the interface and for preserving the good initial MoO_x properties which are deteriorated by the low-temperature annealing.

4. Conclusion

The loss of selectivity with annealing for MoO_x based contacts was addressed. Reducing the MoO_x thickness is important to minimize the solar cells' optical losses - in particular to avoid sub band gap absorption - and to prevent *FF* degradation with annealing. This seems to be the most important step to engineer TMO based SHJ cells towards high efficiencies and high *FF*s and to maintain the initial good selectivity even after annealing.

In addition it was emphasized that the observed non-ideal hole extraction, which occurs already at low-temperature annealing, is clearly linked to the presence of the a-Si:H(i) buffer. The results from pre-annealing the buffer before the MoO_x deposition could not confirm a possible role of hydrogen from the buffer. Another finding is that it is possible to modify the TMOs optical properties by formation of so called gap states as well as their electrical properties, particularly the band bending and selectivity. But none of the pre or post deposition treatments showed a beneficial influence on the selectivity losses with annealing. It was also shown that the induced c-Si junction is one key parameter for the engineering towards a sufficient selectivity. So the major challenge is to maintain the high work function and charges responsible for the induced bend bending during the final annealing of the solar cells.

Acknowledgements

The colleagues at ISE are acknowledged for experimental / technical assistance. The authors especially would like to thank K. Zimmermann, A. Leimenstoll, F. Schätzle, A. Seiler, F. Martin and E. Schäffer for sample preparation and measuring the solar cells. Part of this work has received funding from the European Union's Horizon 2020 research and innovation programme under grant agreement No 727529 Project DISC.

References

[1] Battaglia C, Yin X, Zheng M, Sharp ID, Chen T, McDonnell S, Azcatl A, Carraro C, Ma B, Maboudian R, Wallace RM, Javey A. Hole selective MoOx contact for silicon solar cells. Nano Lett 2014;14:967–71.

[2] Bivour M, Temmler J, Steinkemper H, Hermle M. Molybdenum and tungsten oxide: High work function wide band gap contact materials for hole selective contacts of silicon solar cells. Solar Energy Materials and Solar Cells 2015;142:34–41.

[3] Kostis I, Vourdas N, Papadimitropoulos G, Douvas A, Vasilopoulou M, Boukos N, Davazoglou D. Effect of the Oxygen Sub-Stoichiometry and of Hydrogen Insertion on the Formation of Intermediate Bands within the Gap of Disordered Molybdenum Oxide Films. J. Phys. Chem. C 2013;117:18013–20.

[4] Werner J, Geissbuhler J, Dabirian A, Nicolay S, Morales-Masis M, Wolf S de, Niesen B, Ballif C. Parasitic Absorption Reduction in Metal Oxide-Based Transparent Electrodes: Application in Perovskite Solar Cells. ACS Appl Mater Interfaces 2016;8:17260–7.

[5] Colton RJ, Guzman AM, Rabalais JW. Photochromism and Electrochromism in Amorphous Transition Metal Oxide Films. Accounts of Chemical Research 1978;11:170–6.

[6] Meyer J, Hamwi S, Kroger M, Kowalsky W, Riedl T, Kahn A. Transition metal oxides for organic electronics: energetics, device physics and applications. Adv Mater 2012;24:5408–27.

[7] Greiner MT, Lu Z-H. Thin-film metal oxides in organic semiconductor devices: Their electronic structures, work functions and interfaces. NPG Asia Mater 2013;5:e55.

[8] Vasilopoulou M, Douvas AM, Georgiadou DG, Palilis LC, Kennou S, Sygellou L, Soultati A, Kostis I, Papadimitropoulos G, Davazoglou D, Argitis P. The influence of hydrogenation and oxygen vacancies on molybdenum oxides work function and gap states for application in organic optoelectronics. J Am Chem Soc 2012;134:16178–87.

[9] Geissbühler J, Werner J, Martin de Nicolas S, Barraud L, Hessler-Wyser A, Despeisse M, Nicolay S, Tomasi A, Niesen B, Wolf S de, Ballif C. 22.5% efficient silicon heterojunction solar cell with molybdenum oxide hole collector. Appl. Phys. Lett. 2015;107:81601.

[10] Bivour M, Temmler J, Zahringer F, Glunz S, Hermle M. High work function metal oxides for the hole contact of silicon solar Cells. In: 2016 IEEE 43rd Photovoltaic Specialists Conference (PVSC), p. 215–20.

[11] pv-tools. Available at: http://www.pv-tools.de/products/loana-system/loana-start.html.

[12] Bivour M, Schröer S, Hermle M, Glunz SW. Silicon heterojunction rear emitter solar cells: Less restrictions on the optoelectrical properties of front side TCOs. Solar Energy Materials and Solar Cells 2014;122:120–9.
[13] Pysch D, Meinhard C, Harder N-P, Hermle M, Glunz SW. Analysis and optimization approach for the doped amorphous layers of silicon heterojunction solar cells. Journal of Applied Physics 2011;110:94516.
[14] Sze SM. Semiconductor devices: Physics and technology. 2nd ed. New York: Wiley; 2002.
[15] Würfel P, Würfel U. Physics of solar cells: From basic principles to advanced concepts. 2nd ed. Weinheim: Wiley-VCH; 2010.
[16] Ng KK, Sze SM. Physics of Semiconductor Devices. 3rd ed.: John Wiley & Sons Incorporated; 2006.
[17] Bivour M. Silicon heterojunction solar cells*:* Analysis and basic understanding. PHD thesis, University Freiburg; 2017.
[18] Singh R, Green MA, Rajkanan K. Review of conductor-insulator-semiconductor (CIS) solar cells. Solar Cells 1981;3:95–148.